



Classification and fractal characteristics of coal rock fragments under uniaxial cyclic loading conditions

Yangyang Li¹ · Shichuan Zhang¹ · Xin Zhang¹

Received: 18 September 2017 / Accepted: 9 April 2018 / Published online: 30 April 2018
© Saudi Society for Geosciences 2018

Abstract

Rock burst is a serious geological hazard in deep underground mines affecting progress of mining operations. Although rock burst is a complex process, a distribution law of fractal characteristics can explain the rock failure mechanism. Using a servo-controlled testing system, uniaxial cyclic loading tests on coal rock specimens were conducted to investigate the fractal characteristics of the fragments under different loading rates. To comprehensively characterize the coal fragments of different sizes, samples were divided into four groups of different size: particles, fine, medium-size, and coarse fragments. The distribution of the fragments under uniaxial cyclic loading conditions was then investigated based on the theory of fractal geometry, and the relationships between fractal dimensions and loading rates. Under uniaxial cyclic loading and unloading conditions, most of the fragments are irregular wedges and bulks, exhibiting obvious shape characteristics. Under various loading rates, the length-quantity fractal dimensions of the coal fragments ranged from 0.74 to 1.44, the width-quantity fractal dimensions range from 0.44 to 1.65, and the thickness-cumulative mass fractal dimensions range from 1.0 to 1.33. The coal rock's crushing size-mass fractal dimensions under different loading rates were 2.27, 2.30, 2.32, and 2.35, respectively. Under a small loading rate, the dimension-quantity fractal dimensions are relatively small, suggesting that the coal rock was less crushed, with large fragments differing greatly in length, width, and thickness. The results show that the coal rock fragments exhibit certain shape characteristics after the cyclic loading, like irregular shapes and wedges. Under a larger loading rate, the fragments showed greater fractal dimensions of both size and mass; the coal samples crushed more thoroughly with more uniform fragments in length, width, thickness and mass. The conclusions obtained in this study confirm the classification and fractal characteristics of coal rock fragments by uniaxial cyclic loading conditions in laboratory test and provide the basis for further study on the mechanism of rock burst. This study is helpful for us to make a thorough inquiry the danger degree of rock burst in coal mine by using fractal geometry, understand the effects of methane to coal and the evolution mechanism of cracks, and it can be applied to the research on occurrence mechanism and early warning of rock burst.

Keywords Rock mechanics · Loading rate · Classification statistics · Fractal dimension

Introduction

Coals go through repeated loading and unloading cycles during the mining process. The strength and deformation-induced

failure characteristic of coals under repeated loading affects their long-term stability. It is also important in the investigation and prediction of some dynamic disasters such as rock burst (Wang et al. 2016), coal and gas outbursts (Wold et al. 2008), and water inrush (Wu et al. 2011). Rock burst is a serious geological hazard in deep underground mines affecting progress of mining operations. Although rock burst is a complex process (Akdag et al. 2018), a distribution law of fractal characteristics can explain the rock failure mechanism. At different loading rates, the macro-failure of coal rocks usually starts from the internal defects which go through a grow-expand-accumulate-interconnect process that eventually leads to rock failure. The intrinsic self-similarity of the process results in a post-failure distribution of the fragments with self-similar characteristics, to which fractal geometry theory could

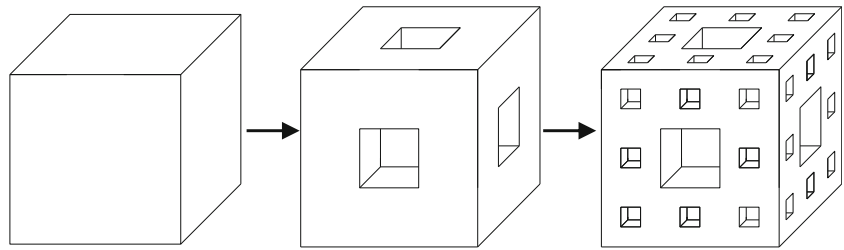
Shichuan Zhang contributed equally to this work.

✉ Shichuan Zhang
373260186@qq.com

Yangyang Li
1161826089@qq.com

¹ State Key Laboratory of Mining Disaster Prevention and Control, Shandong University of Science and Technology, Qingdao 266590, Shandong, China

Fig. 1 Menger sponge model



be applied. So we can use fractal method to study the damage degree of coal samples under different loading rates, further make a thorough inquiry the danger degree of rock burst in coal mine.

Fractal geometry (Engel 1983) focuses on certain irregular curves with self-similarity which, simply put, refers to the characteristic that a substructure resembles a superstructure in the same form. As an effective mathematical tool for the investigation of many irregular and self-similar phenomena in nature, fractal geometry has made its impacts on areas such as electrochemistry (Mahjani et al. 2016), mechanical design (Ángel et al. 2016), urban pattern design (Jevric et al. 2014), and image processing (Bramowicz et al. 2014) since its establishment in 1983. It has been also applied in rock and soil mechanics for the study of key issues including geological structure, rock breakage, and the surface/porosity/joint roughness of rock and soil particles. Certain issues that were previously difficult to define or solve now can be studied with this new approach (Liu et al. 2015, 2016).

The engineering experience (Da et al. 2014) is that, during coal mining and tunnel digging process where coal rocks and the surrounding rocks are typically subjected to repeated loading and unloading cycles, instability may occur, often accompanied with a sudden release of large amount of energy that could trigger dynamic disasters such as rock bursts. This kind of on-site mechanical environment of repeated loads could be reproduced accurately with the cyclic loading and unloading test on the coal samples in the laboratory.

And about the fractal characteristics of fragments under different loading rates, many scholars did a lot of researches. Because they chose different research objects and points, they got different conclusions. For explaining the mechanism of rock burst, Tian et al. (2016) carried out a simulation experiment of rock burst was conducted with the granite samples under a biaxial loading machine system to analyze the fractal characteristics of the fragments from rock burst tests. Hou et al. (2015) examined the dynamic fragmentation of brittle rock by impact experiments using the split Hopkinson pressure bar system and used the generalized extreme value distribution to characterize the size distribution of the fragments. Kong et al. (2016) conducted the triaxial compression experiments of coal sample and found that the amount of gas will cause a variation in the acoustic emission signals and fractal dimension. Many scholars (Sui et al.

2014; Nagahama 2000) found that the post-failure fractal dimension is related to the complexity of cracks in the rocks, i.e., the fractal dimension can serve as a parameter to measure the complexity of coal rock failure. The relationships between fractal dimension and the surface density of fissure, strength, and energy dissipation provide in-depth insight into the rock failure process and energy evolution characteristics under different conditions (distribution patterns of fractures in the rock, loading method, and rate).

However, unlike some dense and homogeneous rocks such as marble, granite, and sandstone, which are the focus of the studies cited above, the coal rocks contain a large number of pre-existing fissures. After being crushed, many fragments with a wide range of sizes are produced, of which the fractal characteristics have been paid little attention. Particularly, the distribution characteristics of coal rock fragments under cyclic loading conditions were never investigated. Therefore, it is necessary to carry out research in fractal characteristics of coal rock fragments under uniaxial cyclic loading conditions.

The purpose of this study was to verify the damage degree of the coal samples under different loading rates; the fractal study of coal fragments as a tool was used; the fractal characteristics of fragments are used to discuss the risk degree of rock burst in coal mine. In this study, we used a MTS815.03 electrohydraulic servo testing system to conduct uniaxial cyclic loading and unloading tests on the coals from Yangcheng Coal Mine, Shandong, China. The coal rock fragments with different sizes were analyzed, the effects of loading rate on the distribution of coal rock fragments were investigated, and the relationships between fractal dimension and loading rate were



Fig. 2 Specimens of coal

Table 1 Coal specimen's basic parameters

Group no.	No.	Height (mm)	Diameter (mm)	Quality (g)	Density (g cm ⁻³)
1#	C11	92.94	48.50	231.53	1.35
	C12	94.12	48.84	235.09	1.33
	C13	95.21	48.76	237.56	1.34
2#	C21	92.38	48.78	232.35	1.35
	C22	96.08	48.66	242.35	1.36
	C23	96.24	48.62	242.68	1.36
3#	C31	95.42	48.72	238.42	1.34
	C32	97.20	48.72	256.21	1.41
	C33	97.36	48.74	266.76	1.47
4#	C41	96.50	48.82	248.34	1.38
	C42	97.68	48.64	267.76	1.48
	C43	95.76	48.78	241.95	1.35

established. The result gives us knowledge on coal rock failure response mechanism under repeated loads, as well as a basic experimental setup/procedure for further investigation of the mechanisms and related catastrophic processes of certain dynamic disasters such as rock burst and explosion.

Calculation of the fractal dimension of the rock fragments

As stated above, although the generated rock fragments with explosion or mechanical actions differ in size and shape, they can all be roughly taken as cuboids in a macroscopic view. From a geometric point of view, the crushing process is a change of cuboid dimensions: the rock is broken into some roughly cubic pieces, some of which are further crushed into even smaller cubic pieces. The formed small rocks with various sizes exhibit a self-similar pattern, i.e., the part is a miniature of whole. This is the fractal characteristics.

Rock structure can be simulated using Menger sponge model (Cieřla and Barbasz 2013) shown in Fig. 1. Constructed based on a certain configuration, the sponge is a complex structure with many pores. Assuming that the initial density of unit cube

is denoted as ρ_0 , the average density of the generated pattern after n iterations is

$$\rho_n = \left(\frac{20}{27}\right)^n \rho_0 \quad (1)$$

when $n \rightarrow \infty$, $\rho_\infty = 0$, suggesting that the actual mass or the volume of Menger sponge is zero. In other words, under certain pressure, the sponge becomes two-dimensional, which means that the solid-looking cube is essentially a partially solid 3D structure whose actual dimension ranges from 2.0 to 3.0. One sees here that, while integer dimensions in classical geometry only give the material's appearance (for example, a stereo structure is 3D while a planar one is 2D), the fractal dimension can better depict the material's intrinsic properties.

Fractal dimension has different definitions, of which the most common one is based on self-similarity and can be expressed as

$$D = -\lim_{\varepsilon \rightarrow 0} \frac{\ln N_\varepsilon}{\ln \varepsilon} \quad \text{or} \quad N_\varepsilon \propto \varepsilon^{-D} \quad (2)$$

where ε denotes the scale, N_ε denotes the measured quantity on this scale, and D denotes the fractal dimension of the object.

If the post-failure rock fragments show a fractal distribution, and the length-quantity, width-quantity, and thickness-quantity show fractal characteristics, the slope of the linear segment of the $\lg N_{L_i} - \lg(L_{\max}/L_i)$ curve is the fractal dimension D of the object. The L_{\max} here denotes the maximum size of the rock fragments in scale space and L_i denotes the characteristic value of the scale size.

As to the calculation of size-quantity fractal characteristics of the rock fragments, the length, width, and thickness of the cuboid fragment can be converted to the equivalent side length L_{eq} of a cube. For some fine particles or micro-particles whose dimensions are hard to measure directly, screening was first performed. Using the particle diameter as the equivalent side

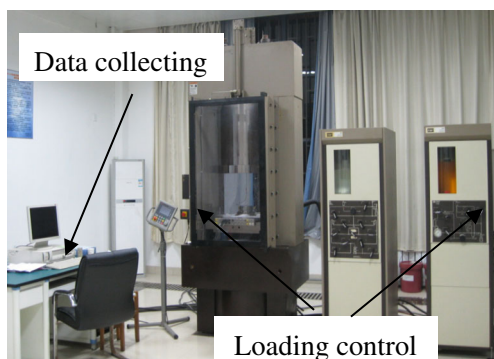
**Fig. 3** MTS815.03 test system

Table 2 Classification standard and analysis method for coal rocks

Fragment category	Size range (mm)	Study methods	Results
Particles	0~0.3	Sieving	Mass distribution Fractal result
	0.3~0.6	Quality weigh	
	0.6~1.0		
	1.0~2.0		
	2.0~5.0		
Fine fragments	5.0~10.0	Quality weigh	Mass distribution Size characteristics Fractal result
	15.0~30.0	Size measurement	
Medium fragments	30.0~50.0	Quality weigh	Mass distribution Size characteristics Fractal result
Coarse fragments	50.0~75.0	Size measurement	

length, particle count statistics was obtained with sampling statistics method. The fractal dimension can be calculated by

$$N = N_0(L_{eq}/L_{eqmax})^{-D} \tag{3}$$

where N denotes the number of fragments with the equivalent side length of the characteristic particle size no smaller than L_{eq} , N_0 denotes the number of fragments with the maximum characteristic size of L_{eqmax} , and D denotes the fractal dimension. When the curve was plotted in log-log coordinate, the slope is the fractal dimension.

If the number of fragments with the diameter over the maximum characteristic size L_{eq} is denoted as $N_{L_{eq}}$, the following expression can be obtained from Eq. (2):

$$N_{L_{eq}} \propto L_{eq}^{-D} \tag{4}$$

$$dN \propto L_{eq}^{-D-1} dL_{eq} \tag{5}$$

If $M_{L_{eq}}$ is the cumulative mass of the fragments with a diameter smaller than L_{eq} and M the total mass of the fragments within the calculation scale, when the fragment

placement obeys Weibull (Wong et al. 2006) distribution, we get

$$\frac{M_{L_{eq}}}{M} = 1 - \exp\left[-\left(\frac{L_{eq}}{\sigma}\right)^b\right] \tag{6}$$

where σ denotes the average size of the rock fragments and b denotes the mass-frequency distribution index. When $(L_{eq}/b)^b \ll 1$, Eq. (6) becomes

$$\frac{M_{L_{eq}}}{M} = -\left(\frac{L_{eq}}{\sigma}\right)^b \tag{7}$$

Since $dM \propto L_{eq}^{-b-1} dL_{eq}$, considering that $dM \propto L_{eq}^3 dN$, we get the size-mass fractal characteristics of the rock fragments as

$$b = \frac{\lg(M_{L_{eq}}/M)}{\lg L_{eq}} \tag{8}$$

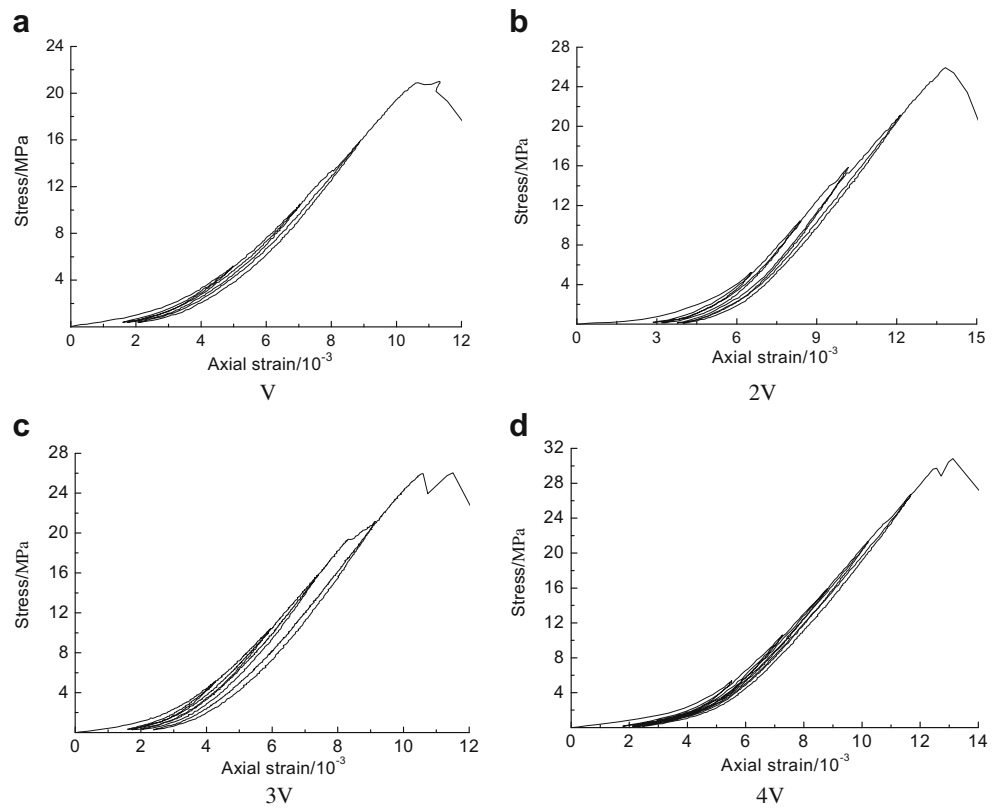
From (8), the fractal dimension is

$$D = 3 - b \tag{9}$$

Table 3 Basic physical and mechanical parameters of coal specimens under different loading rates

Loading rate (kN/s)	Sample no.	No.	Longitudinal wave velocity (m s ⁻¹)	Peak intensity (MPa)	Elastic modulus (GPa)	Peak strain (10 ⁻³)
1	YCM-31	C11	1971.3	23.22	3.15	12.86
	YCM-32	C12	1844.6	24.00	3.24	12.87
	YCM-33	C13	1985.4	21.01	3.04	11.33
2	YCM-34	C21	1875.8	25.93	3.34	13.83
	YCM-35	C22	1920.1	20.77	2.89	12.89
	YCM-36	C23	1886.5	23.24	3.11	12.67
3	YCM-37	C31	1854.2	21.30	2.84	14.39
	YCM-38	C32	1984.3	24.94	3.26	12.13
	YCM-39	C33	1944.6	26.04	3.45	11.50
4	YCM-310	C41	1814.7	25.80	3.31	11.96
	YCM-311	C42	1854.7	30.81	3.53	13.13
	YCM-312	C43	1890.5	26.50	3.13	13.13

Fig. 4 Coal stress-strain curve in axial direction under different loading rates ($V = 1$ kN/s)



where $M_{L_{eq}}/M$ denotes the cumulative percentage content of the fragments with the equivalent length smaller than L_{eq} and $M_{L_{eq}}$ denotes the mass of the fragment with the equivalent length of L_{eq} .

According to the above-described calculation procedure of the fractal dimension D , one should first screen out and weigh the rock fragments from loading-induced failure to get the percentage content of the mass of the fragments with diameters smaller than L_{eq} in total rock mass $M_{L_{eq}}/L_{eq}$; the curve is then plotted in a log-log coordinates ($\lg L_{eq}$ and $\lg(M_{L_{eq}}/L_{eq})$ for x -axis and y -axis, respectively). As long as there is a linear segment in this curve, the fractal characteristics in fragment distribution is confirmed; if multiple linear segments with different slopes are observed, the fragment distribution shows statistical self-similarity on multiple scales. Based on the particle size ranges of various linear segments and the related slopes (b), the non-scale zone of the fragments' fractal distribution and the corresponding fractal dimensions (D) can be calculated according to Eq. (9).

Test conditions and method

Preparation of the specimens

In this study, the coal samples were collected from the third coal seam in the 1302 excavation face of Yangchen Coal

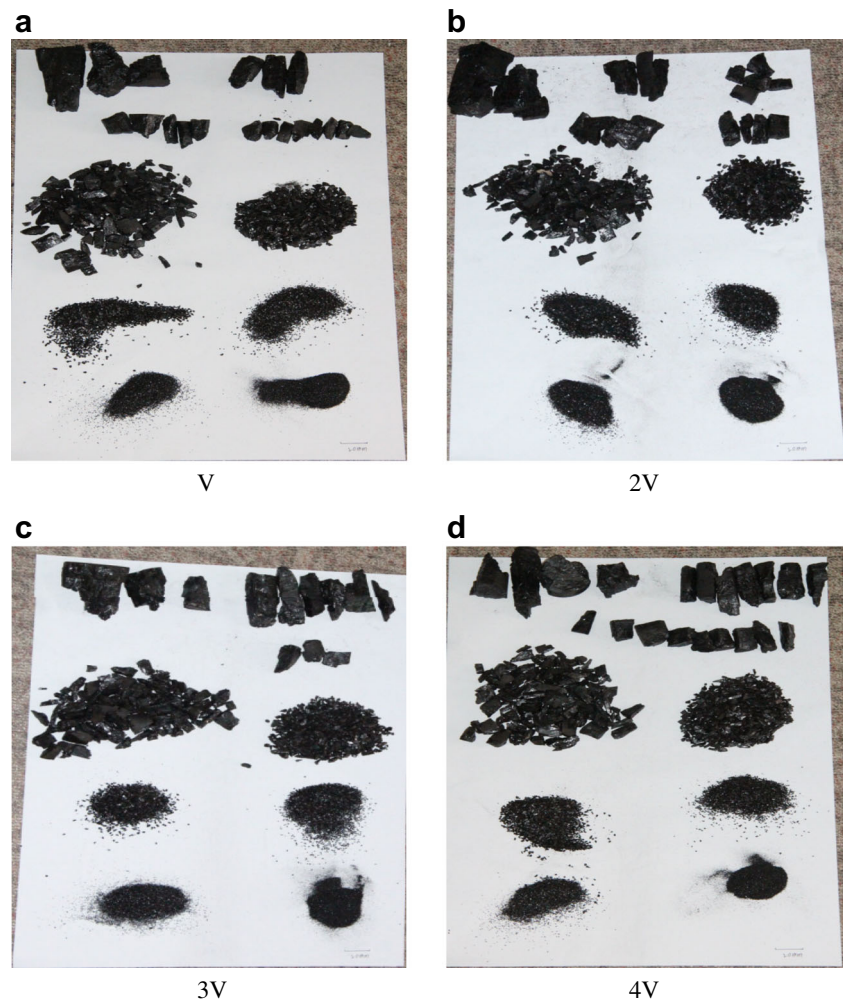
Mine, Shandong Jikuang Luneng Coal and Electricity Co., Ltd. According to the identification result by the Laboratory of Rock Mechanics, Beijing Coal Mining Institute, China Coal Research Institute, this coal seam shows weak outburst proneness. In order to reduce the coal rock's discreteness as much as possible, the intact and unweathered coal rocks of desirable dimensions (length > 200 mm, width and height within 15~20 mm) were collected and sealed on-site before they were carried back to the laboratory for further processing. Figure 2 shows the processed coal specimens, which are $\Phi 50$ mm \times 100 mm with two end faces polished to get parallelism within ± 0.02 mm.

The processed coal specimens were then divided into three groups, each consisting of three specimens. The specimens' size and mass were now accurately measured: each parameter was measured three times to get the average value as the final result. Table 1 lists the coal specimen's basic parameters.

Test system and loading method

In this study, the electrohydraulic servo load test system (MTS815.03) developed by Shandong University of Science and Technology, which is shown in Fig. 3, was used. The maximum axial load is 4600 kN; the horizontal and vertical measuring ranges of the uniaxial extensometer are ± 4 mm and $-2.5 \sim +12.5$ mm, respectively.

Fig. 5 Classification feature of typical samples under different loading rates ($V = 1$ kN/s)



The force loading mode was used. Since the coal specimens are of low strength, the force was gradually stepped up with 10 kN increment until the specimens were completely destroyed. In the loading sequence of $0.5 \rightarrow 10 \rightarrow 0.5 \rightarrow 20 \rightarrow 0.5 \rightarrow 30$ kN, the loading rate was set at 1, 2, 3, and 4 kN/s, respectively. In each set of experiments, three specimens were tested. After the tests, the specimens with loading-induced failures were sealed for further investigation on the size and mass of the fragments.

Fractal statistics of the fragments

Different suitable fractal methods were selected for fragments with different scale ranges. As the abundant pre-existing fractures in coal rocks result in large quantity of fragments smaller than 5 mm, which is hard to measure directly with tools like a vernier caliper, screening method was used to classify these small pieces. For the fragment with the maximum size along any direction over 5 mm, the length, width, and thickness were measured with a vernier caliper. Based on the largest

dimension, the fragments were placed into different groups for different analysis methods.

According to the classification method described in literature (24 Huang 2012), the coal rock fragments were classified into four groups according to the crushing size: particles (smaller than 5 mm), fine fragments (5–30 mm), medium fragments (30–50 mm), and coarse fragments (50–75 mm). Since the number of particles and fine fragments are usually large, for more in-depth characterization, they were further divided into subgroups (five subgroups for particles and two for fine fragments). Table 2 lists the classification standard and analysis method for coal rocks.

Calculation of the fractal dimensions of rock fragments

To comprehensively characterize the fragment distribution under different loading rates, we selected suitable ranges to perform fractal calculation on scale-quantity, crushing size-quantity, and size-mass. It is different from previous research workers (Hou et al. 2015), who often use the equivalent length

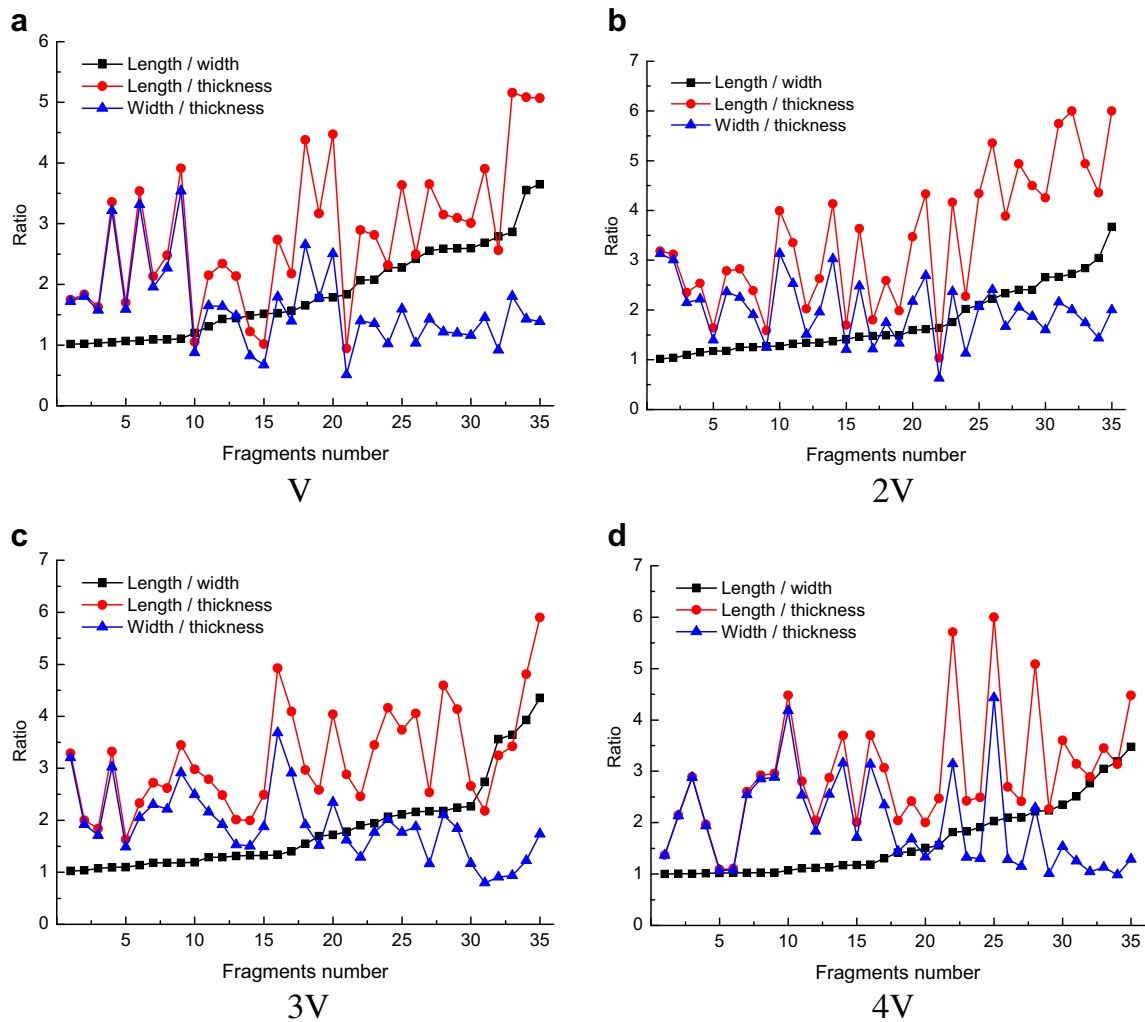


Fig. 6 Size characteristics under uniaxial cyclic loading ($V = 1 \text{ kN/s}$)

to study the fragments characterized. However, it is unable to describe the specific size characteristics of coal fragments. For

Table 4 Length division and quantity under different loading rates

Length/width/ thickness	Section (mm)	Quantity			
		1 kN/s	2 kN/s	3 kN/s	4 kN/s
Length	15.0~30.0	16	17	18	18
	30.0~40.0	7	6	6	9
	40.0~50.0	6	5	5	5
	50.0~60.0	5	5	4	2
	> 60.0	1	2	2	1
Width	10.0~15.0	8	9	13	6
	15.0~18.0	9	5	6	7
	18.0~20.0	6	6	5	8
	20.0~25.0	7	4	7	6
	> 25.0	5	11	4	12
Thickness	1.0~6.0	4	2	2	1
	6.0~10.0	12	18	18	15
	10.0~14.0	10	6	10	12
	14.0~20.0	5	4	2	3
	> 20.0	4	5	3	4

the particles with small size that is hard to measure, sieves are used to divide them into five grades: 0.3, 0.6, 1.0, 2.0, and 5.0 mm; the collected mass of each grade was weighed and recorded for further analysis.

In order to study the fractal characteristics of fragments in detail, there are different size ranges in order to divide zones on different dimensions of length, width, and thickness. Two principles should be followed: firstly, to ensure the scientific data compared with different zones, there is a sufficient amount of coal and rock debris in each zone; secondly, make the distribution of large size fragments more reasonable, and then reduce the influence of the larger size detritus due to the uneven distribution on the test results. For example, if there are no fragments in one range, or most of the fragments mainly concentrate on a particular size range, this will have a very large impact on the test results, and the results will be inaccurate because of the quantity distinct difference. So we require a certain number of fragments in each zone and make the distribution of large size fragments more reasonable.

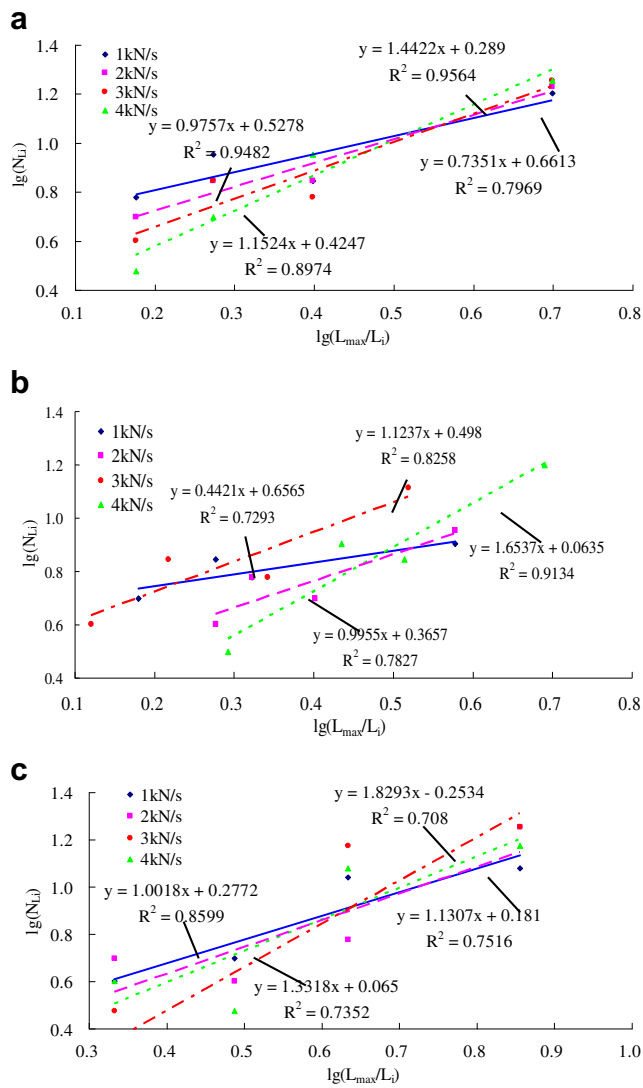


Fig. 7 Logarithmic plot of size-cumulative number under different loading rates. **a** Length logarithmic plot. **b** Width logarithmic plot. **c** Thickness logarithmic plot

Through a large number of different size ranges comparison and analysis, we have determined the optimal scheme to divide zones on different dimensions is determined. The following fragment dimension zones are established for fractal

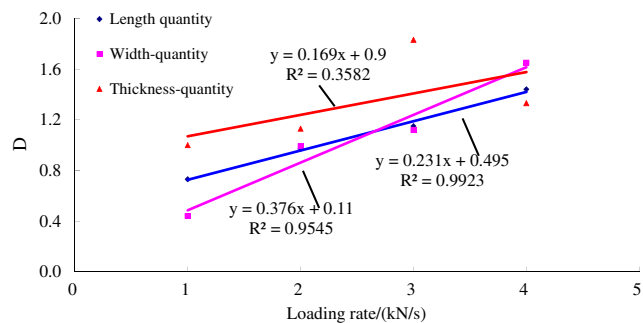


Fig. 8 Fractal dimension of size-cumulative number under different loading rates

Table 5 Partition and quantity of equivalent length under different loading rates

Equivalent length (mm)	Quantity			
	1 kN/s	2 kN/s	3 kN/s	4 kN/s
10.0~17.0	14	17	13	20
17.0~20.0	8	8	10	7
20.0~25.0	5	4	11	7
25.0~35.0	4	4	5	4
> 35.0	3	4	2	2

analysis: for length, 15~30, 30~40, 40~50, 50~60, and over 60 mm; for width, 10~15, 15~18, 18~20, 20~25, and over 25 mm; for thickness, 1~6, 6~10, 10~14, 14~20, and over 20 mm. Fractal dimensions were calculated for length-quantity, width-quantity, and thickness-quantity, respectively. In each scale range, the fractal dimension of size-quantity was calculated according to Eq. (3), and the fractal dimension of equivalent length-mass was calculated with Eqs. (8) and (9).

Results and discussion

Coal rock fragments' size characteristics under different loading rates

Coal rock's stress-strain characteristics under different loading rates

The basic physical and mechanical parameters of the coal rocks under different loading rates are listed in Table 3, which shows that the average peak strengths under these four loading rates are 22.74, 23.31, 24.09, and 27.70 MPa, respectively, while the average peak strains are 0.0124, 0.0131, 0.0129, and 0.0127, respectively. When the loading rate increases, the coal rock strength increases gradually, while the average peak strain follows no obvious change pattern. The average strength of coal rock under cyclic loading test is greater than the value under static uniaxial loading. This can be attributed

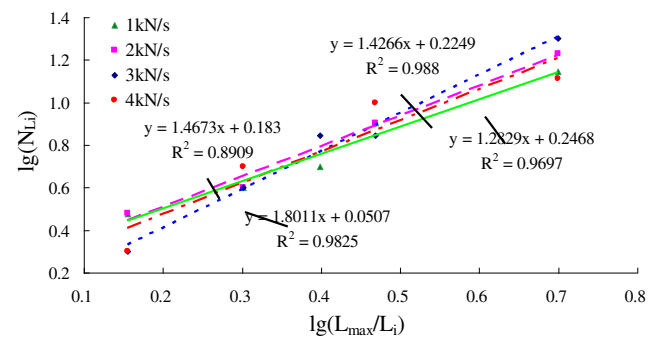


Fig. 9 Logarithmic diagram of equivalent length-number under different loading rates

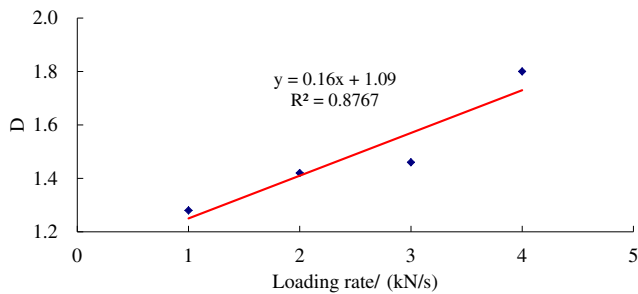


Fig. 10 Fractal dimension of equivalent length-number under different loading rates

to the presence of large number of micro-cracks in coal rocks. Under cyclic loading process, many fine detritus produced with local failures may displaced and find their way into nearby cracks. This helps to increase the friction of the fracture planes in the coal rock to enhance its strength.

The axial stress-strain curves under different loading rates are displayed in Fig. 4, which shows that the curves actually go through the same four stage series: compaction, linear elastic, elastic-plastic, and failure. In all curves, the unloading curve sections go below their corresponding loading ones. The pre-peak strain behaviors, however, differ under different loading rates: under a loading rate of 1 kN/s, the coal rock undergoes post-peak plastic deformation before a quick drop in strength; under a loading rate over 3 kN/s, the curve shows obvious fluctuations (i.e., broken lines) before the peak strength, suggesting the onset of a pseudo-failure phenomenon.

Coal rock’s failure modes under different loading rates

Figure 5 displays the classification features of typical samples (C11, C21, C31, and C41) after failures under different loading rates. From classification features of some typical samples can be found that shape characteristics are evident with the fragments, which are mostly irregular wedges and bulks. As shown in Table 1, each group contains 3 specimens, all

Table 6 Partition and quality of equivalent length under different loading rates

Equivalent length (mm)	Mass greater than equivalent length (g)			
	1 kN/s	2 kN/s	3 kN/s	4 kN/s
0.3	5.3	5.29	5.32	6.06
0.6	8.67	7.07	7.61	9.6
1	10.77	12.09	8.84	13.68
2	44.17	34.21	36.73	48.03
5	139.14	56.16	100.37	120.27
10	77.8	49.08	51.05	85.98
20	98.39	48.71	94.86	112.94
30	130.1	222.68	104.08	89.43

fragments of coal specimens in each group are analyzed after loading failure. The following conclusions are obtained:

1. The coal rock fragments from cyclic loading are characterized by self-similarity.
2. As loading rate increased, the number of the large coal rock fragments decreased gradually, while the numbers of medium-size and small coal rock fragments increased significantly.
3. As the loading rate increases, the sample is crushed more thoroughly, producing more fragments which tend to be flakes with more uniform sizes, smaller masses, and a higher degree of self-similarity.

Coal rock’s shape distribution characteristics under different loading rates

In order to investigate the size characteristics of the coal rock fragments under different loading rates, the lengths, widths, and thicknesses of the fragments were measured by a vernier caliper, so that the length-to-width, length-to-thickness, and width-to-thickness ratios were calculated. Figure 6 shows the calculation results, which were ranked in length-to-width ratio from small to large.

In Fig. 6, the fragment number was named in a certain order of length-to-width ratio from small to large, and the trends of length-to-thickness and length-to-thickness are studied. It can be observed that, the fragment’s size distribution exhibits similar characteristic under different loading rates. With the increase of loading rate, the length-to-width ratio increased gradually at a slow rate; the length-to-thickness increased greatly in a fluctuant way, and the width-to-thickness ratio fluctuates around a certain value while showing a decreasing overall trend.

In combination with the coal rock fragments’ failure morphologies, one sees that, for the coarse fragments, both the width and thickness shrink along with the length, but at smaller rates than that of the length. The length-to-thickness ratio is large, but as the loading rate increases, the drop in thickness is less significant than those of length and width, i.e., the fragments become more like be square flakes.

Coal rock fragment’s fractal characteristics under different loading rates

Scale-quantity fractal dimensions

The specimens were classified into several groups according to their lengths, as shown in Table 4. Figure 7 shows the fractal dimensions of the coal rock’s size-cumulative number under different loading rates, in which the slope is the fractal

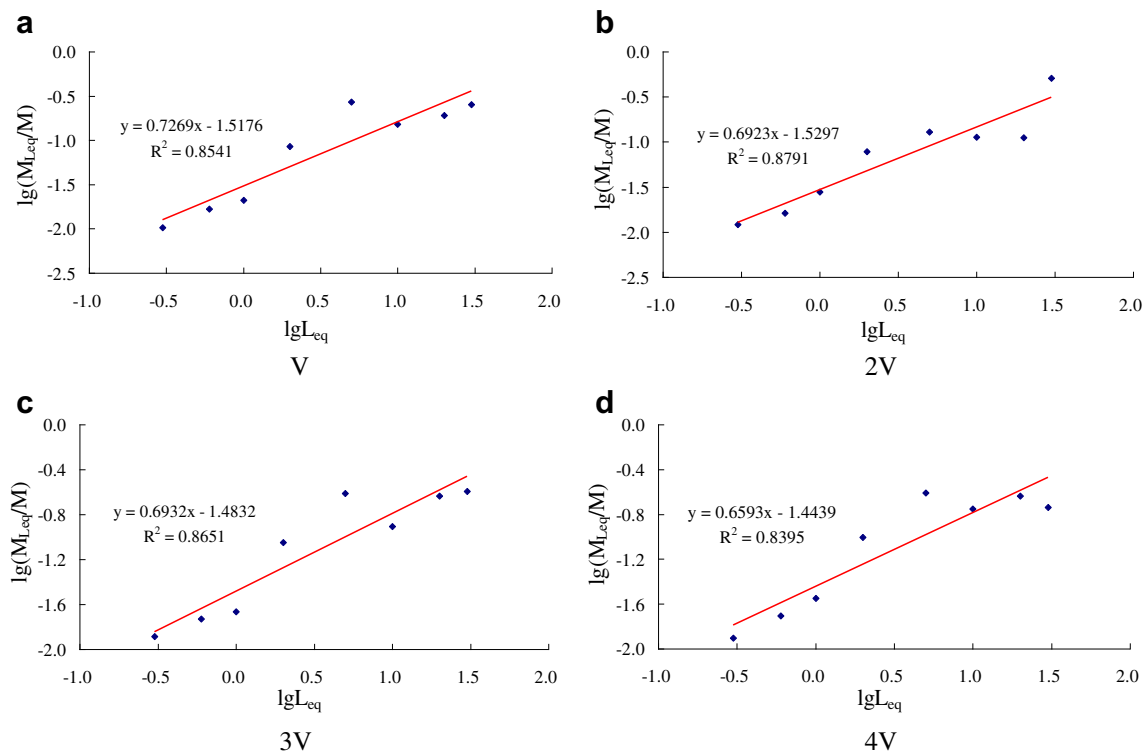


Fig. 11 Logarithmic plot of equivalent length-quality under different loading rates ($V = 1$ kN/s)

dimension and N_{L_i} denotes the cumulative number of the fragments with the length smaller than L_i .

As shown in Fig. 8, the logarithmic size-quantity curves under different loading rates show high goodness of fit. Under different loading rates (1, 2, 3, and 4 kN/s), the fractal dimensions of length-quantity are 0.74, 0.98, 1.15, and 1.44, respectively; for width-quantity, the values are 0.44, 1.0, 1.12, and 1.65, respectively; for thickness-quantity, they are 1.0, 1.13, 1.83, and 1.33, respectively. Under small loading rates, the size-quantity fractal dimensions are small, suggesting that the coal rock had a low crushing degree with fragments large in size and differing greatly in length, width, and thickness. Under a loading rate of 4 kN/s, lots of too-small-to-measure detritus were produced, and the measurable fragments are found mostly in the range of 6–14 mm in thickness, giving a low thickness-quantity fractal dimension.

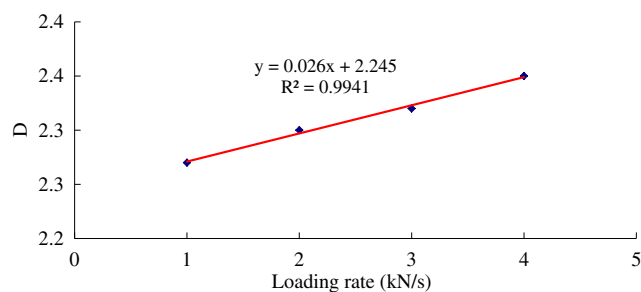


Fig. 12 Fractal dimension of equivalent length-quality under different loading rates

It can be observed from Fig. 7 that the size-quantity fractal dimension increased steadily with the increase of loading rate. Under a greater loading rate, the coal rock shows a higher crushing degree with fragments more uniform in length, width, and thickness.

Fractal dimensions of crushing size-quantity

For a fragment, the equivalent length reflects comprehensively the space occupied by each piece. Table 5 lists the partitioning of the equivalent length and the number of fragments in each range.

Figure 9 shows the logarithmic curves of the fractal dimensions of the equivalent side length-quantity under different loading rates. It can be observed that, under different loading rates (1, 2, 3, and 4 kN/s), the fractal dimensions of equivalent side length-quantity are 1.28, 1.42, 1.46, and 1.8, respectively, as shown in Fig. 10. With the increase of loading rate, the fractal dimension increased gradually, suggesting that the fragment dimensions actually decreased gradually and became more uniform.

Fractal dimensions of crushing size-mass

In this study, the calculated equivalent side lengths of the coal rock fragments ranged from 0.3 to 30 mm. Table. 6 shows the partitioning of the equivalent length and the mass of fragments in each range.

The logarithmic curves of the fractal dimensions of equivalent side length-mass under different loading rates are displayed in Fig. 11. Under different loading rates (1, 2, 3, and 4 kN/s), the fractal dimensions of equivalent side length-mass are 2.27, 2.30, 2.32, and 2.35 from Eq. (9), respectively, as are also shown in Fig. 12. The calculated fractal dimensions increased linearly with the increase of loading rate, suggesting a significant drop in the size of large fragments. The overall decrease in mass is manifested by a shift of the peak mass toward smaller values, accompanied with a shrink in spreading.

It should be noted that this study mainly focused on the coal rock fragments' classification and fractal characteristics under different loading rates, with little attention paid to the destruction process and energy dissipation. In future studies, we will conduct in-depth studies on the coal rock's destruction process and energy evolution under uniaxial cyclic loading conditions to explore the relationship between coal rock's energy dissipation and fragment distribution characteristics under different loading rates.

Conclusions

In this study, the classification and fractal characteristics of the coal rock fragments under different loading rates were investigated using cyclic loading method. The conclusions are as below.

- 1) Under various loading rates, the length-quantity fractal dimensions of the coal fragments ranged from 0.74 to 1.44, the width-quantity fractal dimensions ranged from 0.44 to 1.65, and the thickness-cumulative mass fractal dimensions ranged from 1.0 to 1.33. Under a small loading rate, the dimension-quantity fractal dimensions are relatively small, suggesting that the coal rock was less crushed, with large fragments differing greatly in length, width, and thickness. As the loading rate increased, the specimens were crushed more thoroughly, and the fragments became more uniform in length, width, thickness, and overall size.
- 2) The coal rock's crushing size-mass fractal dimensions under different loading rates are 2.27, 2.30, 2.32, and 2.35, respectively. With the increase of loading rate, the size and mass of large fragments dropped significantly, manifested by a shift of the peak mass toward smaller values, with a tighter spread.
- 3) As the loading rate increased, the fractal dimension of coal fragments increases gradually; the specimens were crushed more thoroughly. It means that the energy released after sample failure, the accumulation of energy before the pre-peak are great. The test results indicated

that the higher the mining or tunneling rate, the more the risk of rock burst.

Author contributions Yangyang Li conceived and designed the experiments and analyzed the data; Shichuan Zhang performed the experiments and wrote the paper.

Funding information This research was financially supported by the Natural Foundation of Shandong Province (ZR2016EEB07), Scientific Research Foundation of Shandong University of Science and Technology Talents (No. 2016RCJJ025), Basic Research Project of Qingdao Source Innovation Program (No. 17-1-1-11-jch), and Taishan Scholar Talent Support Plan for Advantaged & Unique discipline Areas.

Compliance with ethical standards

Conflict of interest The authors declare that they have no conflict of interest.

References

- Akdag S, Karakus M, Taheri A, Nguyen G, Manchao H (2018) Effects of thermal damage on strain burst mechanism for brittle rocks under true-triaxial loading conditions. *Rock Mech Rock Eng* 1–26. doi <https://doi.org/10.1007/s00603-018-1415-3>
- Ángel F-TC, Luis Medina-Monroy J, Lobato-Morales H, Arturo Chávez-Pérez R, Calvillo-Téllez A (2016) A microstrip antenna based on a standing-wave fractal geometry for cubesat applications. *Microw Opt Technol Lett* 58(9):2210–2214
- Bramowicz M, Kulesza S, Czaja P, Maziarz W (2014) Application of the autocorrelation function and fractal geometry methods for analysis of images. *Arch Metall Mater* 59(2):451–457
- Cieřla M, Barbasz J (2013) Random packing of spheres in Menger sponge. *J Chem Phys* 138(21):214704
- Da H, Tan Q, Huang R (2014) Fractal characteristics of fragmentation and correlation with energy of marble under unloading with high confining pressure. *Chin J Rock Mech Eng* 31(7):1379–1389
- Engel P (1983) The fractal geometry of nature (book review). *Sciences* 23:63–68
- Hou T, Xu Q, Zhou J (2015) Size distribution, morphology and fractal characteristics of brittle rock fragmentations by the impact loading effect. *Acta Mech* 226(11):3623–3637
- Jevric M, Knezevic M, Kalezic J, Kopitovic-Vukovic N, Cipranic I (2014) Application of fractal geometry in urban pattern design. *Tehnicki Vjesnik* 21(4):873–879
- Kong X, Wang E, Hu S, Shen R, Li X, Zhan T (2016) Fractal characteristics and acoustic emission of coal containing methane in triaxial compression failure. *J Appl Geophys* 124:139–147
- Liu R, Jiang Y, Li B, Wang X (2015) A fractal model for characterizing fluid flow in fractured rock masses based on randomly distributed rock fracture networks. *Comput Geotech* 65:45–55
- Liu R, Li B, Jiang Y (2016) A fractal model based on a new governing equation of fluid flow in fractures for characterizing hydraulic properties of rock fracture networks. *Comput Geotech* 75:57–68
- Mahjani M, Moshrefi R, Sharifi-Viand A, Taherzad A, Jafarian M, Hasanlou F (2016) Surface investigation by electrochemical methods and application of chaos theory and fractal geometry. *Chaos, Solitons Fractals* 91:598–603
- Nagahama H (2000) Fractal scalings of rock fragmentation. *Earth Sci Fron* 7(1):169–177

- Sui L, Yang Y, Ju Y (2014) Fractal description of rock fracture behavior. *Mec Pract* 36:753–756
- Tian B, Liu S, Zhang Y, Wang Z (2016) Analysis of fractal characteristic of fragments from rock burst tests under different loading rates. *Tehnicki Vjesnik* 23:1269–1276
- Wang G, Gong S, Li Z, Dou L, Cai W, Mao Y (2016) Evolution of stress concentration and energy release before rock bursts: two case studies from Xingan coal mine, Hegang, China. *Rock Mech Rock Eng* 49(8):3393–3401
- Wold M, Connell L, Choi S (2008) The role of spatial variability in coal seam parameters on gas outburst behaviour during coal mining. *Int J Coal Geol* 75(1):1–14
- Wong T-f, Wong RHC, Chau KT, Tang CA (2006) Microcrack statistics, Weibull distribution and micromechanical modeling of compressive failure in rock. *Mech Mater* 38(7):664–681
- Wu Q, Liu Y, Yang L (2011) Using the vulnerable index method to assess the likelihood of a water inrush through the floor of a multi-seam coal mine in China. *Mine Water Environ* 30(1):54–60